Usefulness of Gadobenate Dimeglumine - Enhanced Hepatobiliary Phase MR Imaging on Predicting Histological Grade of Hepatocellular Carcinoma

Sung Ho Park, Myeong-Jin Kim, Jin-Young Choi, Joon Seok Lim, Ki Whang Kim

Purpose : To assess the usefulness of gadobenate dimeglumine-enhanced hepatobiliary phase MR imaging for evaluation of histological characteristics of hepatocellular carcinoma (HCC).

Materials and Methods : 57 HCCs histopathologically proved by surgery in 51 patients were retrospectively evaluated. All patients underwent gadobenate dimeglumine-enhanced MR imaging prior to surgery. The signal-to-noise ratio (SNR) of lesion and liver, and the liver-to-lesion contrast-to-noise ratio (CNR) for both pre- and postcontrast hepatobiliary phase were measured and contrast enhancement ratio (CER) of lesion and liver were calculated to correlate with three groups stratified by histological grades (Edmondson-Steiner classification) of the lesions. The differences between means of each group were statistically analyzed with one-way analysis of variance test.

Results : The liver-to-lesion CNRs of well-differentiated HCCs (n=9) on pre- (−0.8±13.2) and postcontrast hepatobiliary phase images (13.2±30.4) were significantly lower ($p<0.05$) compared to those of moderately (14.2±9.4 and 39.1±15.4 on pre- and postcontrast, respectively) (n=37) and poorly differentiated HCCs (18.6±11.3 and 39.3±27.9) (n=11), respectively. There were no significant difference for CERs between three histological tumor grades.

Conclusion : Gadobenate dimeglumine-enhanced hepatobiliary phase MR imaging can help predict the histological grades of hepatocellular carcinomas preoperatively, especially differentiating well- from moderately and poorly differentiated HCCs.

Index words : Hepatocellular carcinoma
Magnetic resonance imaging
Gadobenate dimeglumine
Histological grade
Hepatobiliary phase

JKSMRM 15:208-218(2011)

Department of Radiology, Research Institute of Radiological Science, Institute of Gastroenterology, Yonsei University College of Medicine

Received; October 10, 2011, revised; October 18, 2011, accepted; October 25, 2011

Corresponding author : Myeong-Jin Kim, M.D., Department of Diagnostic Radiology, Yonsei University College of Medicine, 250 Seongsan-no, Seodaemun-gu, Seoul 120-752, Korea.
Tel. 82-2-2228-7400 Fax. 82-2-393-3035 E-mail: kimnex@yuhs.ac

Introduction

Characterization for focal liver tumors on MRI using various contrast agents has become more and more important at the present time as well as lesion detection, since accurate diagnosis and early and appropriate treatment could provide a better prognosis and also increase curability (1–5). In this regard, gadobenate dimeglumine (Gd-BOPTA; MultiHance, Bracco SpA, Milan, Italy) might be one of the most useful contrast agents because Gd-BOPTA is a gadolinium-based paramagnetic contrast agent which has combined properties of a conventional extracellular fluid (ECF) contrast agent with those of a liver-specific contrast agent and can provide combination of dynamic and liver-specific imaging (6, 7). As for the dynamic imaging, prior studies for the clinical value of gadolinium chelates demonstrated dynamic imaging showed good performance for characterization of focal liver lesions and for detection of hypervascular hepatic tumors (8, 9). 3∼5% of the injected dose of Gd-BOPTA is taken up by the functioning hepatocytes and excreted in bile (6, 10). Gd-BOPTA has twofold higher T1-relaxivity than conventional gadolinium chelates and shows marked and prolonged enhancement of the liver parenchyma up to 2 hour on T1-weighted images (11, 12), so that delayed phased imaging of Gd-BOPTA can be obtained 1∼2 hours after venous administration of the contrast agent. These characteristics provide radiological usefulness to differentiate hepatocyte-origin tumors from non-hepatocyte-origin tumors (13, 14) as well as increased detectability for focal liver lesions in a background of strongly enhancing liver parenchyma (7, 10–12, 15–17).

There have been several previous studies which have revealed that Gd-BOPTA-enhanced MR imaging has superior diagnostic value in an attempt to detect and characterize hepatocellular carcinoma (HCC) and delayed phase imaging of Gd-BOPTA provide additional information for the characterization of HCC (13, 14, 16–20). On delayed phase imaging, HCC, one of the most common hepatocyte-origin malignant tumor, shows wide variation in liver-to-lesion contrast-to-noise ratio (CNR) on previous investigations by Manfredi et al (13), Grazioli et al. (14), and Kim et al. (18). It is thought that multiple intrinsic and extrinsic factors might affect this variation. However, until now, there has been insufficient study data about efficacy of the delayed phase imaging using Gd-BOPTA in patients who have HCC with histopathological correlation. The purposes of this study were to evaluate histological characteristics of HCC and identify the factors which might affect the liver-to-lesion CNR using Gd-BOPTA-enhanced hepatobiliary phase MR imaging.

Materials and Methods

Patient population

51 patients who underwent hepatic resection and Gd-BOPTA-enhanced MR imaging 1 month prior to surgical resection of the tumor between August 2005 and June 2007 were included in this study. 43 patients were male and 8 female, with a mean age of 56 years (range 25–70 years). A total of 57 HCC nodules were confirmed by surgical resection and histopathology and retrospectively evaluated. Excluded from the study were patients who had a history of prior transcatheter arterial chemoembolization (TACE) or radiofrequency ablation (RFA). Histological analysis was performed on the lesion and liver. Edmonson-Steiner classification was used for evaluating histological grades of the HCCs. Other pathological findings of the HCCs were analyzed with histological types (trabecular, pseudoglandular, compact, scirrhous), cell types (hepatic, clear, giant, spindle), bile formation, and fat and iron deposition of the HCCs. The degree of liver function was based on the Child-Pugh classification, with all patients classified as having Child-Pugh class A cirrhosis. Total bilirubin levels were within the normal range (0.2–1.2 mg/dL) in 50 patients. The bilirubin level was slightly elevated in one patient (1.6 mg/dL).

MRI examination

All MR imaging was performed using a 1.5-T imaging system (Achieva 1.5T Nova Dual, Philips Medical Systems, Best, Netherlands) with four-channel phased-array body coils (Synergy; Philips Medical Systems, Best, Netherlands). The liver was imaged in the axial planes both before and after administration of Gd-BOPTA. The MRI protocol consisted of a breath-hold transverse T1-weighted in- and out-of-phase two-dimensional gradient-echo (2D-GRE) sequence (TR/in phase TE, 150/2.4 msec; TR/out-of-phase TE, 150/1.2;

matrix, 256×256; section thickness, 6 mm; slice spacing, 1.2 mm), a single-slice T2-weighted fast spin-echo (TR/TE, 466/148 msec; matrix, 288×230, section thickness, 4 mm; slice spacing, 1 mm) with spectral fat suppression technique, and breath-hold T1-weighted three-dimensional gradient-echo (3D-GRE) sequences for precontrast, postcontrast dynamic, and postcontrast hepatobiliary phase (TR/TE, 4.7/2.3 msec; matrix, 320×224; slice thickness, 3 mm; no gap). Contrast-enhancing MRI was performed after the intravenous administration of a total dose of 0.1 mmol/kg body weight Gd-BOPTA. To determine the optimal timing for the hepatic arterial phase fluoroscopic bolus detection technique was used in all patients. Portal venous, hepatic venous, and equilibrium phase images were obtained approximately 20–30 seconds after the acquisition of the prior phase images. Hepatobiliary phase images were obtained between 120 and 180 minutes after the intravenous administration of Gd-BOPTA.

Image analysis

Quantitative analysis was performed on T1-weighted 3D-GRE images obtained before and after the administration of Gd-BOPTA. We measured the liver signal intensity, tumor signal intensity, and the standard deviation of the background noise using operator-defined regions of interest (ROIs) for each image. The ROI of the lesion was positioned to avoid the necrotic foci and blood vessels and background noise was measured just ventral to the right anterior abdominal wall where the respiratory or motion-related artifact was absent. Based on the values recorded, the signal-to-noise ratio (SNR) of lesion and liver, the liver-to-lesion contrast-to-noise ratio (CNR) for both pre- and postcontrast heptaobiliary phases, and contrast enhancement ratio (CER) of lesion and liver were calculated to correlate with histological characteristics of lesion and liver according to the following equations:

$$SNR_{liver} = SI_{liver} / SD_{noise}\ ,\ SNR_{lesion} = SI_{lesion} / SD_{noise}$$
$$CNR = (SI_{liver} - SI_{lesion}) / SD_{noise}$$
$$CER\ (\%) = [\ (SNR\ post - SNR\ pre) / SNRpre\ ]$$

Where SI_{lesion} is the signal intensity of the lesion; SI_{liver} is the signal intensity of the liver parenchyma; and SD_{noise} is the standard deviation of the background noise. The size of lesion was also evaluated.

Statistical analysis

The differences between means of each group were statistically analyzed with one-way analysis of variance (ANOVA) test and Student's t test. The level for significance was $p<0.05$. The statistical analyses were performed using SPSS computer software (SPSS, version 12.0, SPSS, Chicago).

Results

All HCCs were stratified with three groups according to Edmonson-Steiner classification and there were 9 well-, 37 moderately, and 11 poorly differentiated HCCs. The size of the tumors ranged from 1.0 to 9.5 cm with a mean size of 3.5 cm (well-differentiated HCCs, 2.3±1.7; moderately differentiated HCCs, 3.6±2.6; poorly differentiated HCCs, 4.4±2.7). The SNR of lesion and liver, the liver-to-lesion CNR for both pre- and postcontrast hepatobiliary phase, the CER of lesion and liver of three groups are shown in Table 1. The

Table 1. Results of Quantitative Analysis Regarding the Signal-to-Noise Ratio (SNR) of Lesion and Liver, the Liver-to-Lesion Contrast-to-Noise Ratio (CNR), and Contrast Enhancement Ratio (CER) of Lesion and Liver

		Grade I	Grade II	Grade III
Precontrast	SNR (Lesion)	49.3±14.1	44.5±24.8	32.7±12.6
	SNR (Liver)	48.6±9.0	58.6±29.0	51.2±21.7
	CNR	−0.8±13.2*	14.2±9.4	18.6±11.3
Postcontrast	SNR (Lesion)	88.1±33.8*	62.1±26.7	48.8±16.9
	SNR (Liver)	101.3±25.4	101.2±33.9	87.1±42.2
	CNR	13.2±30.4*	39.1±15.4	38.3±27.9
	CER (Lesion)	0.8±0.4	0.5±0.5	0.5±0.3
	CER (Liver)	1.1±0.4	0.9±0.5	0.7±0.5

* vs Grade II and III ; significantly different ($p<0.05$) using ANOVA

mean value of the liver-to-lesion CNR of well-differentiated HCCs (−0.8±13.2) was significantly lower ($p<0.05$) than those of moderately (14.2±9.4) and poorly differentiated HCCs (18.6±11.3) on precontrast scans (Fig. 1a). We also found significant difference ($p<0.05$) in the mean value of the liver-to-lesion CNR of well-differentiated HCCs (13.2±30.4) compared to those of moderately (39.1±15.4) and poorly differenti-ated HCCs (38.3±27.9) on post-contrast hepatobiliary phase (Fig. 1b). The mean value of the SNR of well-differentiated HCCs (88.1±33.8) was significantly higher ($p<0.05$) than those of moderately (62.1±26.7) and poorly differentiated HCCs (48.8±16.9) on postcontrast hepatobiliary phase.

The mean value of CER of lesion also tended to be higher in patients with well-differentiated HCCs, but its statistical differences with moderately and poorly differentiated HCCs were not significant ($p=0.18$ and 0.43, respectively).

For histological types of HCCs, only compact type tumor showed significantly higher liver-to-lesion CNR (49.3±18.0, $p<0.05$) on postcontrast hepatobiliary phase images compared to those of non-compact type (31.4±20.3) (Table 2). Other various histopathological characteristics with cell types, bile formation, and fat deposition of HCCs showed no significant difference for liver-to-lesion CNR on both pre- and post-contrast 3D-GRE images and CER of lesion (Tables 3, 4). But we

Table 2. Liver-to-Lesion Contrast-to-Noise Ratio (CNR) on Pre- and Postcontrast Images and Contrast Enhancement Ratio (CER) of Lesion for Various Histological Types of Hepatocellular Carcinoma

	Trabecular (n=52)	Pseudoglandular (n=21)	Compact (n=10)	Scirrhous (n=7)
	Non-Trabecular (n=2)	Non-Pseudoglandular (n=33)	Non-Compact (n=44)	Non-Scirrhous (n=47)
Precontrast CNR	13.3±10.6 9.2±15.5	14.4±9.3 12.3±11.4	10.7±11.0 13.7±10.6	15.0±6.2 12.8±11.1
Postcontrast CNR	34.0±20.8 54.0±20.0	30.6±17.5 37.3±22.7	49.3±18.0* 31.4±20.3	35.4±15.2 34.6±21.8
CER (Lesion)	0.5±0.4 0.5±0.2	0.6±0.5 0.5±0.4	0.6±0.4 0.5±0.4	0.4±0.3 0.6±0.4

* vs Non-compact type postcontrast CNR ; significantly different ($p<0.05$) using t test

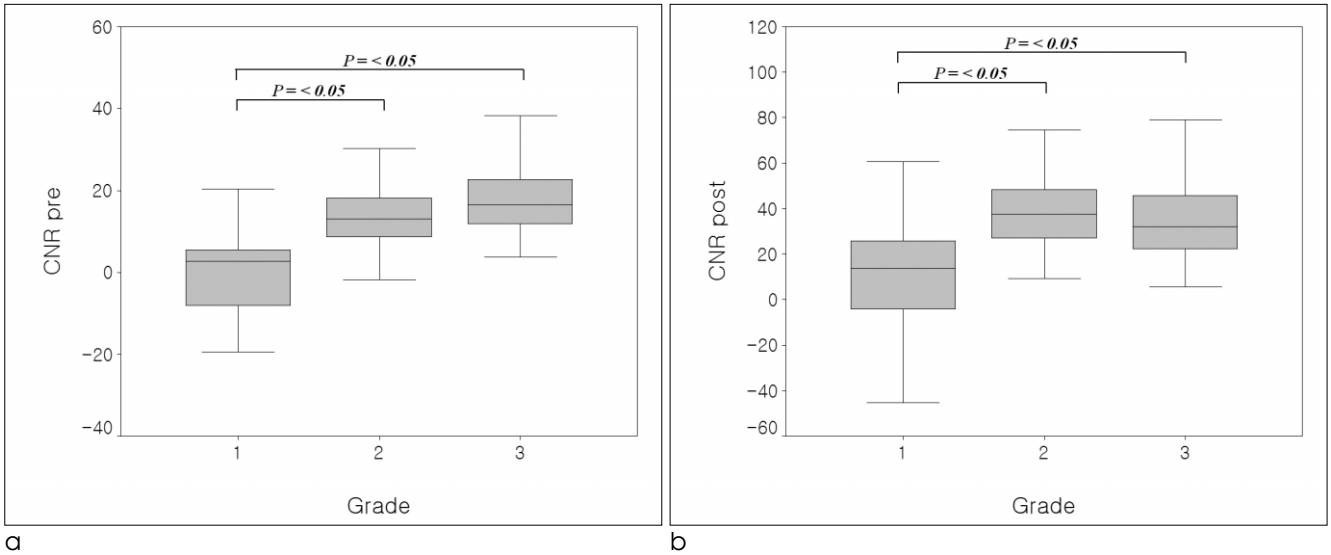

a b

Fig. 1. The liver-to-lesion contrast-to-noise ratio (CNR) of well- (grade 1), moderately (grade 2), and poorly differentiated (grade 3) hepatocellular carcinomas on precontrast (a) and postcontrast hepatobiliary T1-weighted three dimensional-gradient echo images (b).

observed intralesional bile which might express residual hepatocytic activity of the lesion was present in 2/9 (22.2%) well-differentiated HCCs and 3/37 (8.1%) moderately differentiated HCCs, while poorly differentiated HCCs did not represent intralesional bile at all. Only one lesion had iron deposition (precontrast CNR −6.5, postcontrast CNR 25.7, CER 0.6), thus statistical analysis could not be accomplished.

Discussion

Our study demonstrated that the liver-to-lesion CNR of well-differentiated HCCs on pre- and postcontrast hepatobiliary T1-weighted 3D-GRE images were

Table 4. Liver-to-Lesion Contrast-to-Noise Ratio (CNR) on Pre- and Postcontrast Images and Contrast Enhancement Ratio (CER) of Lesion for Other Pathological Findings of Hepatocellular Carcinoma

	Bile Formation (n=5) Non-Bile Formation (n=50)	Fat Deposition (n=14) Non-Fat Deposition (n=42)
Precontrast CNR	11.9±9.3 13.7±11.2	10.4±11.8 14.1±11.1
Postcontrast CNR	36.6±16.8 35.7±22.9	28.8±25.8 37.8±20.7
CER (Lesion)	0.8±0.3 0.5±0.4	0.4±0.4 0.6±0.4

Table 3. Liver-to-Lesion Contrast-to-Noise Ratio (CNR) on Pre- and Postcontrast Images and Contrast Enhancement Ratio (CER) of Lesion for Various Cell Types of Hepatocellular Carcinoma

	Hepatic (n=51) Non-Hepatic (n=3)	Clear (n=14) Non-Clear (n=41)	Giant (n=8) Non-Giant (n=47)	Spindle (n=2) Non-Spindle (n=54)
Precontrast CNR	13.6±11.2 12.2±12.1	12.4±8.8 14.0±11.8	16.1±9.6 28.0±11.1	27.4±13.2 12.7±11.0
Postcontrast CNR	34.0±22.0 58.3±16.0	39.0±15.1 34.7±24.3	28.1±11.1 37.1±23.5	36.6±10.5 35.5±22.6
CER (Lesion)	0.5±0.4 0.5±0.1	0.6±0.4 0.5±0.4	0.4±0.3 0.6±0.4	0.8±0.1 0.6±0.4

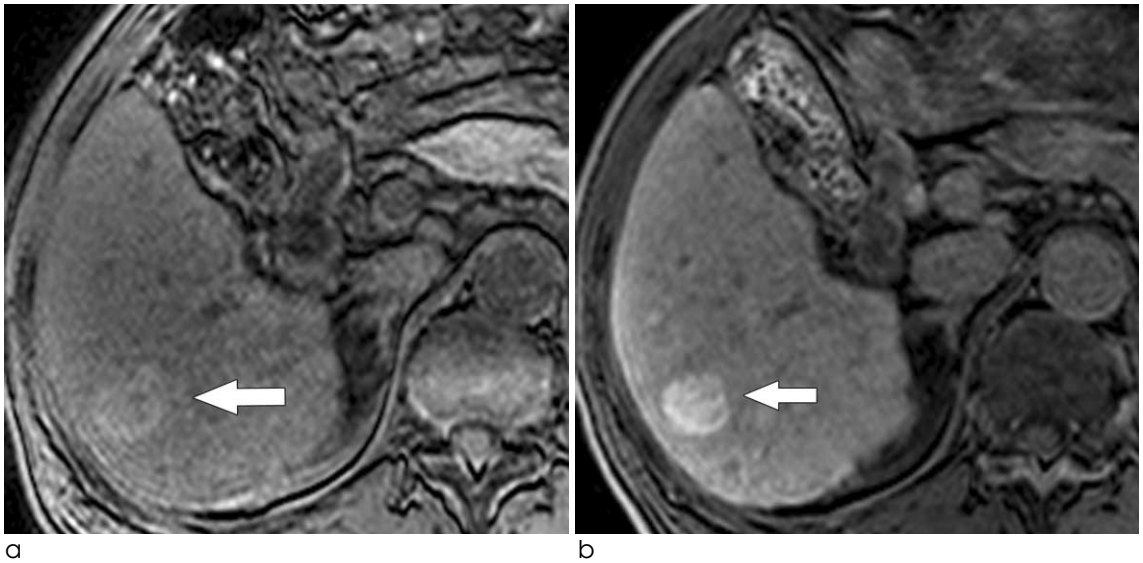

a b

Fig. 2. A 65-year-old patient with well-differentiated HCC. (a) Precontrast T1-weighted three-dimentional gradient-echo image shows a slightly hyperintense signal mass (arrow) in the right lobe of the liver. (b) Gadobenate dimeglumine-enhanced hepatobiliary phase image demonstrates the lesion (arrow) shows markedly increased uptake of the contrast agent. Consequently the liver-to-lesion CNR of lesion on postcontrast hepatobiliary phase has a negative value.

significantly lower compared to those of moderately and poorly differentiated HCCs, respectively (Table 1 & Fig. 1). Low CNR means that the difference of SNRs between lesion and liver is not significant and the conspicuity of the lesion is poor in terms of lesion detection. Therefore results in our study suggest that the conspicuity of the lesion on both pre- and postcontrast hepatobiliary images in patients with well-differentiated HCCs is worse than moderately and poorly differentiated HCCs (Figs. 2–5).

There are many elements which affects the lesion conspicuity of HCCs on precontrast or postcontrast MR imaging of liver: the functionality of the normal hepatic parenchyma; composition and degree of vascularization

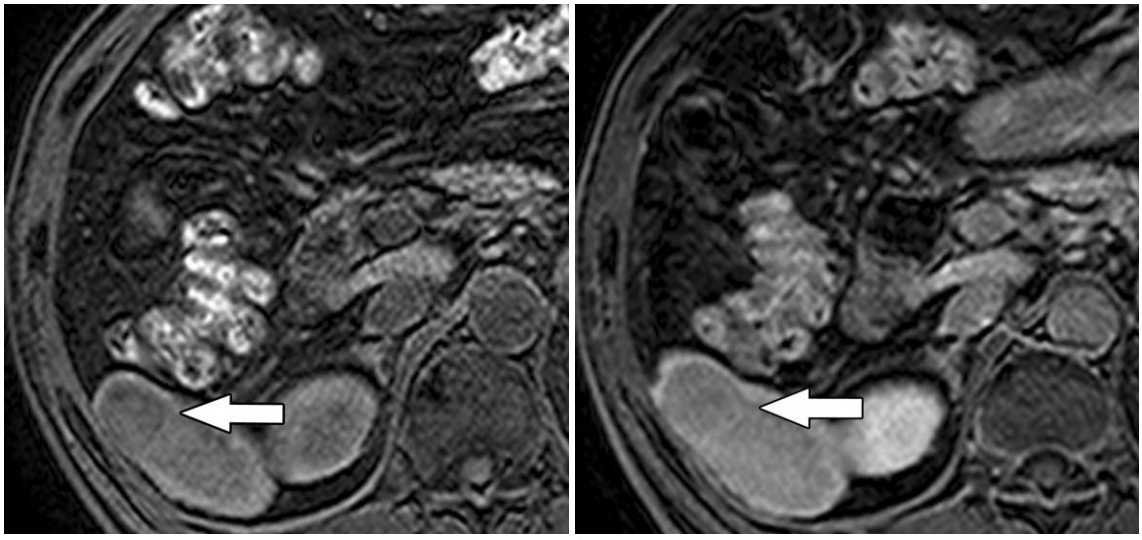

a b

Fig. 3. A 52-year-old patient with well-differentiated HCC. (a) Precontrast T1-weighted three-dimentional gradient-echo image shows a slightly hypointense signal mass (arrow) in the right lobe of the liver. (b) Gadobenate dimeglumine-enhanced hepatobiliary phase image demonstrates the lesion (arrow) shows slightly hypointense to surrounding liver parenchyma. Thus the lesion-to-liver CNR of lesion on postcontrast hepatobiliary phase has a low positive value.

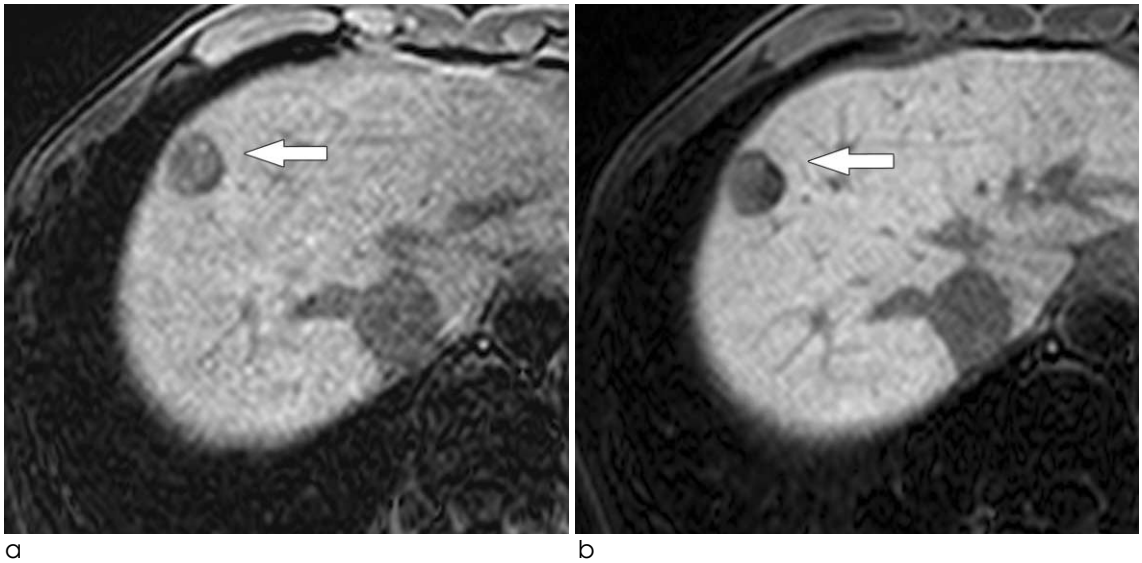

a b

Fig. 4. A 54-year-old patient with moderately differentiated HCC. (a) Precontrast T1-weighted three-dimentional gradient-echo image shows that a mass (arrow) in the right lobe of the liver has apparent hypointense signal intensity. (b) Gadobenate dimeglumine-enhanced hepatobiliary phase image demonstrates the lesion (arrow) is markedly hypointense signal intensity to surrounding liver parenchyma.

of the lesion; the residual hepatic functionality of the neoplastic cells themselves; and so on (14, 20–22). Unfortunately, such factors tend to vary from patient to patient, often making the behavior of a given lesion difficult to predict. The results of previous studies aimed at correlating the appearance of HCC on MR imaging with the pathological characteristics of the lesion reflect the difficulty in drawing firm conclusions on the behavior of such lesions (1, 5, 23–25).

In our study, the mean CNR of well-differentiated HCCs would be partly related with the slightly higher mean SNR of lesion than that of liver for precontrast images (Fig. 2a). Our results of precontrast images are comparable with those reported by Yamashita et al. (24) and Kadoya et al. (23) for correlation of MR imaging and histopathological findings of HCCs. They demonstrated well-differentiated HCCs have a tendency to be hyperintense on precontrast T1-weighted images, while moderately or poorly differentiated HCCs to be hypointense. Hyperintensity on precontrast T1-weighted images could be significantly related with composition of the tumor cells such as fat or paramagnetic ions deposition, hemorrhagic portion, and so on. However, we could not conclude these results were the specific characteristics of well-differentiated HCCs for precontrast images because there were no statistical significance of the SNR of lesion for precontrast images between tumor grades in our study (Table 1) as Kadoya et al. (23) also speculated in which hyperintensity on precontrast T1-weighted images is a feature of hyperplastic changes of the hepatocytes.

There has been prior reports investigating the role of the hepatobiliary contrast agents on the lesion detection and characterization in relation with the histopathological findings of HCCs, especially the histological grades (Edmondson-Steiner classification) (6, 13, 14, 20). Some of these reports (13, 14, 20) demonstrated the poorly differentiated HCC nodules appeared more hypointense to the surrounding enhanced liver parenchyma, whereas the well-differentiated ones tended to show similar or greater enhancement on postcontrast hepatobiliary phase. Manfredi et al. (13) reported that well-differentiated HCC might show more enhancement (superior contrast enhancement ratios) than poorly differentiated HCC and similarly Murakami et al. (6) also reported. Our results on postcontrast hepatobiliary phase are in good agreement with those of former reports. The mean SNR of lesion of well-differentiated HCCs was significantly higher than those of moderately and poorly differentiated HCCs on postcontrast hepatobiliary images in the present study (Table 1). These results affected the mean CNR of well-

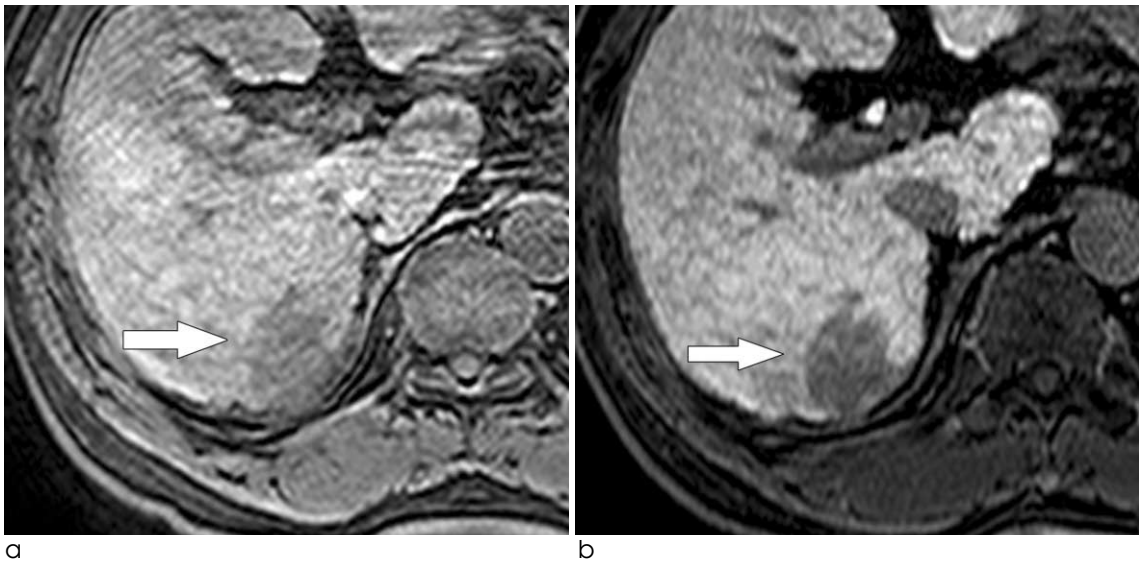

a b

Fig. 5. A 56-year-old patient with poorly differentiated HCC. (a) Precontrast T1-weighted three-dimentional gradient-echo image shows that a mass (arrow) in the right lobe of the liver has apparent hypointense signal intensity. (b) Gadobenate dimeglumine-enhanced hepatobiliary phase image demonstrates the lesion (arrow) is markedly hypointense to surrounding liver parenchyma.

differentiated HCCs which was significantly lower than those of moderately and poorly differentiated HCCs (Fig. 1b). The CER of lesion also tended to be higher on the well-differentiated HCCs, although its differences with those of moderately and poorly differentiated HCCs were not statistically significant. In only three cases, the CNRs on postcontrast hepatobiliary images were negative (maximum −45.2, minimum −4.1, and mean −17.9) and all three cases were included only in the group of the patients with well-differentiated HCCs (Fig. 2b). This is one of the reasons that could explain the lower mean CNR of well-differentiated HCCs, however not the only one. The mean value of the remaining positive CNRs on well-differentiated HCCs (maximum 60.9, minimum 8.8, and mean 28.7) is also lower than those of moderately and poorly differentiated HCCs. These findings obtained with Gd-BOPTA for well-differentiated HCCs in the present study could be affected by several factors reported in prior studies (4, 13, 14, 26, 27). They suggested that the residual hepatocytic activity of hepatocellular lesion allows the lesion to take up Gd-BOPTA and consequently to increase its signal intensity, therefore reducing the CNR. Intralesional bile could be one of the indicators expressing retention of sufficient hepatocytic functionality of the lesion. Grazioli et al. (14) reported that a significant positive correlation between the presence of intralesional bile and the degree of enhancement of the lesions after Gd-BOPTA administration in their study. Although no significant difference was observed between CER and bile formation in our study (Table 4), some well- and moderately differentiated HCCs represented intralesional bile (22.2%, 8.1%), while poorly differentiated HCCs did not at all. Moreover, low postcontrast CNR could be affected by other factors such as the presence of fat or paramagnetic ions (iron, copper) (21, 22), but the effect of fat deposition on the liver-to-lesion CNR for postcontrast hepatobiliary phase in our study was not statistically significant. Statistical analysis for iron deposition could not be accomplished because of small sample size (only one lesion having iron).

The tendency for moderately differentiated HCCs to show greater enhancement than well-differentiated HCCs on postcontrast hepatobiliary images of Gd-BOPTA was explained as a result of the larger size of moderately differentiated HCCs than that of well-differentiated HCCs (6.3±3.4 cm vs. 3.8±1.8 cm) in the report by Grazioli et al. (14), but we observed the tendency for greater enhancement of well-differentiated HCCs compared with moderately differentiated HCCs nevertheless moderately differentiated HCCs showed larger size than that of well-differentiated HCCs (3.6±2.6 cm vs. 2.3±1.7 cm) similar to their report. Among the prior mentioned residual hepatocytic activity of hepatocellular lesion and histopathological characteristics such as intralesional bile, fat or paramagnetic ions deposition, the size of the lesion, and intralesional fibrous stroma (14, 18, 20), our study results favor the residual hepatocytic activity of the lesion representing as intralesional bile might be the most important factor to explain Gd-BOPTA uptake of the lesion on postcontrast hepatobiliary images than any other factors.

As a liver-specific MR imaging contrast agent recently introduced for clinical imaging, gadoxetate disodium (gadolinium-ethoxybenzyl-diethylenetriamine pentaacetic acid; Gd-EOB-DTPA) is highly liver specific in the hepatobiliary phase, appropriately 20 minutes after injection, with an uptake of about 50% by the organic anion-transporting polypeptide 1 (28–30). There are also previous preclinical and clinical studies that found a tendency toward greater enhancement in well-differentiated HCCs over moderately and poorly differentiated HCCs in hepatobiliary phase using Gd-EOB-DTPA (27, 31–33), as our study did. Although subtle differences exist between the results of these studies, we could conclude that some well-differentiated HCCs and a few moderately differentiated HCCs might show mild to moderate accumulation of Gd-EOB-DTPA in hepatobiliary phase. Narita et al. (34) observed a strong correlation between enhancement ratios and expression levels of organic anion-transporting polypeptide 1B3 protein of HCCs so they reported uptake of Gd-EOB-BOPTA in HCCs is determined by the expression of this transporter rather than tumor differentiation. Kitao et al. (35) and Tsuboyama et al. (36) also explained tumor enhancement by expression patterns of sinusoidal and canalicular transporters. Compared with the results of our study and others, further evaluation is needed to determine the relationship, if any, between tumor grade and expression of transporters.

Our study had several limitations. First of all, we could not consider the relationship with the degree of liver failure because all patients in our study were classified as having Child-Pugh class A cirrhosis and most patients had normal ranges of bilirubin levels. Limited patient population of our study results from clinical situation that Child-Pugh class B or C cirrhosis are not usually surgical candidates. Grazioli et al. (14) demonstrated that there was a positive correlation between the degree of liver failure and the worsening of liver-to-lesion CNR on postcontrast hepatobiliary phase. The results of prior study by Kim et al. (37) substantiate these findings. In our study, the SNR of liver on both precontrast and postcontrast hepatobiliary phase and the CER of liver showed no statistical significance between histological tumor grades and this observed enhancement characteristics of liver parenchyma might be different in Child-Pugh class B and C cirrhosis. Secondly, we did not compare the performance of Gd-BOPTA postcontrast hepatobiliary images with dynamic images of nonspecific extracellular contrast agents. We believe that further study with comparison between Gd-BOPTA-enhanced MR imaging and extracellular gadolinium chelates-enhanced MR imaging will be necessary. Lastly, there might have been a potential selection bias in our patient population due to the retrospective nature of this study.

In conclusion, gadobenate dimeglumine-enhanced hepatobiliary phase MR imaging can help predict the histological grades of HCCs, especially differentiating well-differentiated HCCs from moderately and poorly differentiated HCCs, thus may have clinical efficacy for the planning of surgical treatment and the assessment of the patient's prognosis as estimating the histological grades of HCCs preoperatively.

References

1. Ebara M, Ohto M, Watanabe Y, et al. Diagnosis of small hepatocellular carcinoma: correlation of MR imaging and tumor histologic studies. Radiology 1986;159:371-377
2. Karhunen PJ. Benign hepatic tumours and tumour like conditions in men. J Clin Pathol 1986;39:183-188
3. McGahan JP, Browning PD, Brock JM, Tesluk H. Hepatic ablation using radiofrequency electrocautery. Invest Radiol 1990;25:267-270
4. Ni Y, Marchal G, Zhang X, et al. The uptake of manganese dipyridoxal-diphosphate by chemically induced hepatocellular carcinoma in rats. A correlation between contrast-media-enhanced magnetic resonance imaging, tumor differentiation, and vascularization. Invest Radiol 1993;28:520-528
5. Earls JP, Theise ND, Weinreb JC, et al. Dysplastic nodules and hepatocellular carcinoma: thin-section MR imaging of explanted cirrhotic livers with pathologic correlation. Radiology 1996;201:207-214
6. Murakami T, Baron RL, Peterson MS, et al. Hepatocellular carcinoma: MR imaging with mangafodipir trisodium (Mn-DPDP). Radiology 1996;200(1):69-77
7. Kirchin MA, Pirovano GP, Spinazzi A. Gadobenate dimeglumine (Gd-BOPTA). An overview. Invest Radiol 1998;33:798-809
8. Spinazzi A, Davies A, Tirone P, Rosati G. Predictable and unpredictable adverse reactions to uroangiographic contrast media. Acad Radiol 1996;3 Suppl 2:S210-213
9. Yu JS, Kim MJ, Kim KW, et al. Hepatic cavernous hemangioma: sonographic patterns and speed of contrast enhancement on multiphase dynamic MR imaging. AJR Am J Roentgenol 1998;171:1021-1025
10. Vogl TJ, Pegios W, McMahon C, et al. Gadobenate dimeglumine--a new contrast agent for MR imaging: preliminary evaluation in healthy volunteers. AJR Am J Roentgenol 1992;158:887-892
11. Grazioli L, Kirchin M, Pirovano G, Spinazzi A. MultiHance in the dynamic phase of contrast enhancement: a pictorial assessment. J Comput Assist Tomogr 1999;23 Suppl 1:S61-64
12. Caudana R, Morana G, Pirovano GP, et al. Focal malignant hepatic lesions: MR imaging enhanced with gadolinium benzyloxypropionictetra-acetate (BOPTA)--preliminary results of phase II clinical application. Radiology 1996;199:513-520
13. Manfredi R, Maresca G, Baron RL, et al. Delayed MR imaging of hepatocellular carcinoma enhanced by gadobenate dimeglumine (Gd-BOPTA). J Magn Reson Imaging 1999;9:704-710
14. Grazioli L, Morana G, Caudana R, et al. Hepatocellular carcinoma: correlation between gadobenate dimeglumine-enhanced MRI and pathologic findings. Invest Radiol 2000;35:25-34
15. Spinazzi A, Lorusso V, Pirovano G, Taroni P, Kirchin M, Davies A. Multihance clinical pharmacology: biodistribution and MR enhancement of the liver. Acad Radiol 1998;5 Suppl 1:S86-89; discussion S93-94
16. Petersein J, Spinazzi A, Giovagnoni A, et al. Focal liver lesions: evaluation of the efficacy of gadobenate dimeglumine in MR imaging--a multicenter phase III clinical study. Radiology 2000;215:727-736
17. Pirovano G, Vanzulli A, Marti-Bonmati L, et al. Evaluation of the accuracy of gadobenate dimeglumine-enhanced MR imaging in the detection and characterization of focal liver lesions. AJR Am J Roentgenol 2000;175:1111-1120
18. Kim YK, Lee JM, Kim CS. Gadobenate dimeglumine-enhanced liver MR imaging: value of dynamic and delayed imaging for the characterization and detection of focal liver lesions. Eur Radiol 2004;14:5-13
19. Peterson MS, Baron RL, Murakami T. Hepatic malignancies:

usefulness of acquisition of multiple arterial and portal venous phase images at dynamic gadolinium-enhanced MR imaging. Radiology 1996;201:337-345
20. Vogl TJ, Stupavsky A, Pegios W, et al. Hepatocellular carcinoma: evaluation with dynamic and static gadobenate dimeglumine-enhanced MR imaging and histopathologic correlation. Radiology 1997;205:721-728
21. Ebara M, Watanabe S, Kita K, et al. MR imaging of small hepatocellular carcinoma: effect of intratumoral copper content on signal intensity. Radiology 1991;180:617-621
22. Kitagawa K, Matsui O, Kadoya M, et al. Hepatocellular carcinomas with excessive copper accumulation: CT and MR findings. Radiology 1991;180:623-628
23. Kadoya M, Matsui O, Takashima T, Nonomura A. Hepatocellular carcinoma: correlation of MR imaging and histopathologic findings. Radiology 1992;183:819-825
24. Yamashita Y, Fan ZM, Yamamoto H, et al. Spin-echo and dynamic gadolinium-enhanced FLASH MR imaging of hepatocellular carcinoma: correlation with histopathologic findings. J Magn Reson Imaging 1994;4:83-90
25. Winter TC, 3rd, Takayasu K, Muramatsu Y, et al. Early advanced hepatocellular carcinoma: evaluation of CT and MR appearance with pathologic correlation. Radiology 1994;192: 379-387
26. Manfredi R, Maresca G, Baron RL, et al. Gadobenate dimeglumine (BOPTA) enhanced MR imaging: patterns of enhancement in normal liver and cirrhosis. J Magn Reson Imaging 1998;8:862-867
27. Ni Y, Marchal G, Yu J, Muhler A, Lukito G, Baert AL. Prolonged positive contrast enhancement with Gd-EOB-DTPA in experimental liver tumors: potential value in tissue characterization. J Magn Reson Imaging 1994;4:355-363
28. Hamm B, Staks T, Muhler A, et al. Phase I clinical evaluation of Gd-EOB-DTPA as a hepatobiliary MR contrast agent: safety, pharmacokinetics, and MR imaging. Radiology 1995;195:785-792
29. Schuhmann-Giampieri G, Schmitt-Willich H, Press WR, Negishi C, Weinmann HJ, Speck U. Preclinical evaluation of Gd-EOB-DTPA as a contrast agent in MR imaging of the hepatobiliary system. Radiology 1992;183:59-64
30. van Montfoort JE, Stieger B, Meijer DK, Weinmann HJ, Meier PJ, Fattinger KE. Hepatic uptake of the magnetic resonance imaging contrast agent gadoxetate by the organic anion transporting polypeptide Oatp1. J Pharmacol Exp Ther 1999; 290:153-157
31. Vogl TJ, Kummel S, Hammerstingl R, et al. Liver tumors: comparison of MR imaging with Gd-EOB-DTPA and Gd-DTPA. Radiology 1996;200:59-67
32. Reimer P, Rummeny EJ, Daldrup HE, et al. Enhancement characteristics of liver metastases, hepatocellular carcinomas, and hemangiomas with Gd-EOB-DTPA: preliminary results with dynamic MR imaging. Eur Radiol 1997;7:275-280
33. Huppertz A, Haraida S, Kraus A, et al. Enhancement of focal liver lesions at gadoxetic acid-enhanced MR imaging: correlation with histopathologic findings and spiral CT--initial observations. Radiology 2005;234:468-478
34. Narita M, Hatano E, Arizono S, et al. Expression of OATP1B3 determines uptake of Gd-EOB-DTPA in hepatocellular carcinoma. J Gastroenterol 2009;44:793-798
35. Kitao A, Zen Y, Matsui O, et al. Hepatocellular carcinoma: signal intensity at gadoxetic acid-enhanced MR imaging--correlation with molecular transporters and histopathologic features. Radiology 2010;256:817-826
36. Tsuboyama T, Onishi H, Kim T, et al. Hepatocellular carcinoma: hepatocyte-selective enhancement at gadoxetic acid-enhanced MR imaging--correlation with expression of sinusoidal and canalicular transporters and bile accumulation. Radiology 2010;255:824-833
37. Kim JI, Lee JM, Choi JY, et al. The value of gadobenate dimeglumine-enhanced delayed phase MR imaging for characterization of hepatocellular nodules in the cirrhotic liver. Invest Radiol 2008;43:202-210

대한자기공명의과학회지 15:208-218(2011)

Gadobenate Dimeglumine 조영증강 간담도기 자기공명영상을 이용한 간세포암의 병리학적 분화도 예측

연세대학교 의료원 영상의학교실 영상의학연구소 소화기연구소

박성호 · 김명진 · 최진영 · 임준석 · 김기황

목적 : 간세포암의 조직학적 특성과의 비교평가를 통해 gadobenate dimeglumine 조영증강 간담도기 자기공명영상의 유용성을 평가하였다.

대상 및 방법 : 수술 전 gadobenate dimeglumine 조영증강 자기공명영상을 실시한 후 수술을 통해 조직학적으로 확진된 51명 57개의 간세포암을 대상으로 후향적 연구를 하였다. 조영 전 및 후 간담도기에서 병변 및 간의 신호대잡음비와 간-병변 대조도대잡음비를 측정하였으며 병변 및 간의 대조도증강비를 계산하여 조직학적으로 세 군으로 분류된 병변들과 비교분석을 실시하였다. 각각의 군간 평균값 차이를 일원분산분석을 통해 통계적으로 분석하였다.

결과 : 고분화도 간세포암의 조영 전 및 후의 간-병변 대조도대잡음비 (-0.8±13.2, 13.2±30.4) 가 중등도 (14.2±9.4, 39.1±15.4) 및 저분화도 간세포암 (18.6±11.3, 39.3±27.9) 에 비해 각각 통계적으로 유의하게 낮았다 ($p < 0.05$).

결론 : Gadobenate dimeglumine 조영증강 간담도기 자기공명영상은 수술 전에 간세포암의 조직학적 분류를 예측하는데 도움을 줄 수 있다.

통신저자 : 김명진, (120-752) 서울시 서대문구 성산로 250, 연세대학교 의료원 영상의학교실 영상의학연구소 소화기연구소
Tel. (02)2228-7400 Fax. (02)393-3035 E-mail: kimnex@yuhs.ac